

New aspects of Doppler imaging in Sun-as-a-star observations

A. M. Broomhall^{1*}, W. J. Chaplin¹, Y. Elsworth¹, R. New²

¹*School of Physics and Astronomy, University of Birmingham, Edgbaston, Birmingham B15 2TT*

²*Faculty of Arts, Computing, Engineering and Sciences, Sheffield Hallam University, Sheffield S1 1WB*

ABSTRACT

Birmingham Solar Oscillations Network (BiSON) instruments use resonant scattering spectrometers to make unresolved Doppler velocity observations of the Sun. Unresolved measurements are not homogenous across the solar disc and so the observed data do not represent a uniform average over the entire surface. The influence on the inhomogeneity of the solar rotation and limb darkening has been considered previously (Brookes et al. 1978a) and is well understood. Here we consider a further effect that originates from the instrumentation itself. The intensity of light observed from a particular region on the solar disc is dependent on the distance between that region on the image of the solar disc formed in the instrument and the detector. The majority of BiSON instruments have two detectors positioned on opposite sides of the image of the solar disc and the observations made by each detector are weighted towards differing regions of the disc. Therefore the visibility and amplitudes of the solar oscillations and the realization of the solar noise observed by each detector will differ. We find that the modelled bias is sensitive to many different parameters such as the width of solar absorption lines, the strength of the magnetic field in the resonant scattering spectrometer, the orientation of the Sun’s rotation axis, the size of the image observed by the instrument and the optical depth in the vapour cell. We find that the modelled results best match the observations when the optical depth at the centre of the vapour cell is 0.55. The inhomogeneous weighting means that a ‘velocity offset’ is introduced into unresolved Doppler velocity observations of the Sun, which varies with time, and so has an impact on the long-term stability of the observations.

Key words: methods: observational, Sun: helioseismology, Sun: oscillations

1 INTRODUCTION

Birmingham Solar Oscillations Network (BiSON) instruments use resonant scattering spectrometers to make unresolved observations of the Sun (Brookes et al. 1978b). This involves determining the intensity of light scattered by a potassium vapour into the blue and red wings of a solar Fraunhofer line. If the solar Fraunhofer line is Doppler shifted the intensities observed on the blue and red wings will not be equal and this difference allows the line-of-sight velocity between the Sun and the instrument to be determined. Since BiSON instruments make unresolved observations the intensity recorded in each wing is integrated over the entire solar disc. Brookes et al. (1978a) showed that, because of the solar rotation and limb darkening, unresolved observations are not homogenous across the solar disc and so the observed data do not represent a uniform average over the entire surface.

Here we consider a further influence on the Doppler imaging that originates from the instrumentation itself. The key component of each BiSON instrument is a cell containing potassium vapour. The intensity of light observed from a particular region on the solar disc is dependent on the position of the detector with respect to the

image of the solar disc that is formed in the cell. The majority of BiSON instruments have two detectors, called port and starboard, which are positioned on opposing sides of the observed solar image. In this paper we demonstrate that observations made by each detector are weighted towards differing regions of the solar disc. This has consequences for the visibility of the modes and the coherency of the data observed from the two detectors.

The layout of the rest of this paper is as follows. We begin, in Section 2, by giving a brief description of the BiSON instrumentation. Then, in Section 3, we use this information to model the bias across the solar disc that is seen in unresolved Doppler velocity observations. We have modelled the effect of the solar rotation and limb darkening, both of which have been considered previously (Brookes et al. 1978a), and we show that the observed bias is also dependent on the position of the detector with respect to the image of the Sun captured by an instrument. The line-of-sight velocity between the Sun and an instrument is constantly varying due to the Earth’s orbital and spin velocities and in Section 4 we determine the effect of this variation on the raw measured data. We also investigate how sensitive the model results are to various input parameters, such as the width of the solar absorption line, the width and separation of the instrumental absorption lines, the position angle of the Sun’s rotation axis, the size of the image seen

* E-mail: amb@bison.ph.bham.ac.uk

by the instrument and the optical depth of the vapour in the instrument's cell. The total observed line-of-sight velocity between the Sun and an instrument is determined by calculating a ratio of intensities. Comparisons are made between the observed and modelled ratios to obtain estimates of the optical depth in the vapour cell and the size of the image of the Sun observed by an instrument. We then use the observed and modelled ratios to determine a 'velocity offset' that is present in the BiSON data (Section 5). We aim to model this velocity offset as it affects the long-term stability of the BiSON observations and introduces noise into the data. The main results of this paper and consequences of the observed Doppler imaging are discussed in Section 6.

2 BISON INSTRUMENTATION

BiSON observations are made using resonant scattering spectrometers, which determine the magnitude of Doppler velocity shifts in the solar potassium Fraunhofer line at 769.9 nm (Brookes et al. 1978b). Potassium vapour is enclosed in a vapour cell and placed in a magnetic field, typically of strength 0.18 T, which corresponds to a separation in the left- and right-circularly polarized Zeeman components of the laboratory emission line of 0.013 nm. This is equivalent to a Doppler shift of 5200 m s^{-1} . The right-circularly polarized Zeeman component is shifted to a longer wavelength and so will be referred to as the red instrumental component in the remainder of this paper. The left-circularly polarized Zeeman component is shifted to a shorter wavelength and so will be referred to as the blue instrumental component. The two shifted instrumental components are located on opposing wings of the potassium solar Fraunhofer line.

In addition to any oscillation velocities that might be observed, the total observed line-of-sight velocity between the Sun and the instrument, v_{obs} , contains several components: the velocity due to the Earth's orbit around the Sun, v_{orb} , the velocity due to the Earth's spin on its own axis, v_{spin} , the gravitational redshift, v_{grs} , and various other offsets, collectively known as v_{other} , which include the Doppler imaging offset that will be discussed in this paper and any offsets due to noise. The BiSON group uses the JPL ephemeris look-up tables, which are available through the JPL Horizons system, to determine the sum of the line-of-sight velocity due to v_{orb} and v_{spin} . We define the 'station velocity', v_{st} , as the sum of these two velocities, i.e.,

$$v_{\text{st}} = v_{\text{orb}} + v_{\text{spin}}. \quad (1)$$

To determine the observed Doppler velocity of the Sun with respect to the instrument, v_{obs} , the following ratio is calculated from the raw observations:

$$R = \frac{I_b - I_r}{I_b + I_r}, \quad (2)$$

where I_b and I_r are the observed strengths of the resonantly scattered signal on the blue and red sides of the solar line, respectively. At small line-of-sight velocities the blue and red instrumental components are positioned on the parts of the solar absorption line with the steepest gradient, making the measurements very sensitive to small changes in line-of-sight velocity. However at large line-of-sight velocities the instrumental components are positioned on shallower portions of the solar absorption line, thus reducing the sensitivity of the measurements. In other words, the sensitivity is dependent on the magnitude of the line-of-sight velocity between the Sun and the instrument.

We model the relationship between the station velocity, v_{st} , and the ratio, R , with the following equation:

$$R(v_{\text{st}}) = \sum_{i=0}^N a_i v_{\text{st}}^i, \quad (3)$$

where N is the order of the polynomial and a_i are the coefficients of the polynomial. The order of the polynomial must be chosen carefully. If there the number of terms included is too small there are insufficient degrees of freedom in the model to follow the change in sensitivity throughout the day. However, if too many terms are included in the polynomial the fit becomes unstable and the signal from the oscillations can be lost when the series is subtracted from the measured values. Currently, when the BiSON data are processed, a cubic ($N = 3$) polynomial is used (Elsworth et al. 1995). A best fit algorithm is used to determine the coefficients, a_i , in equation 3 and the gravitational redshift, v_{grs} , on a day-by-day basis. In the remainder of this paper, when modelling the observed Doppler imaging, we take $v_{\text{grs}} = 632 \text{ m s}^{-1}$. This is marginally higher than the offset measured by the instruments, as it does not account for the observed convective blue shift, but it is a good approximation. The modelled ratio, given by equation 3, is subtracted from the observed ratio, as defined by equation 2, to leave a residual from which the oscillation velocities can be determined.

We now use this information about the manner in which BiSON instruments measure velocity shifts to determine the observed bias across the solar disc.

3 MODELLING THE BIAS ACROSS THE DISC

Figure 1 shows the weighting of the solar disc caused by limb darkening and the solar rotation. This work has been performed previously by Brookes et al. (1978a) but is included here so that the weightings can be compared with those observed when we take into account instrumental effects (in Section 3.1). The weightings shown in Figure 1 are scaled relative to the region that contributes most to the unresolved observations. So a weighting of 100 corresponds to the region that contributes most to the unresolved observations and a weighting of 50 corresponds to a region that contributes half of the maximum. Contours with weightings from 30 to 90 have been plotted.

The Sun's rotation axis was taken to be vertical and the period of rotation was taken as the constant value of 25 days, which corresponds to the observed rotation period of the material at the solar equator. The Sun actually exhibits differential rotation, such that the rotation period of material at the poles is approximately 36 days and so assuming a uniform rotation at all latitudes is rather simplistic. However, increasing the rotation period to 36 days has a negligible effect on the calculated bias, implying the results would not be altered significantly by the inclusion of differential rotation. The rotation of the Sun is in an anti-clockwise direction if viewed from above, looking down on the north pole (north is upwards in Figure 1). Therefore, in Figure 1, the left solar limb is approaching an observer on Earth, while the right solar limb is receding.

As can be seen in Figure 1 observations made with the red instrumental wing are weighted most heavily towards the approaching limb of the solar disc, while observations made with the blue instrumental wing are most heavily weighted towards the receding solar limb. This is expected as BiSON spectrometers observe a narrow absorption line and so, for example, the blue instrumental wing observes a larger intensity of light from regions of the solar disc that are red shifted i.e. the receding limb of the solar disc.

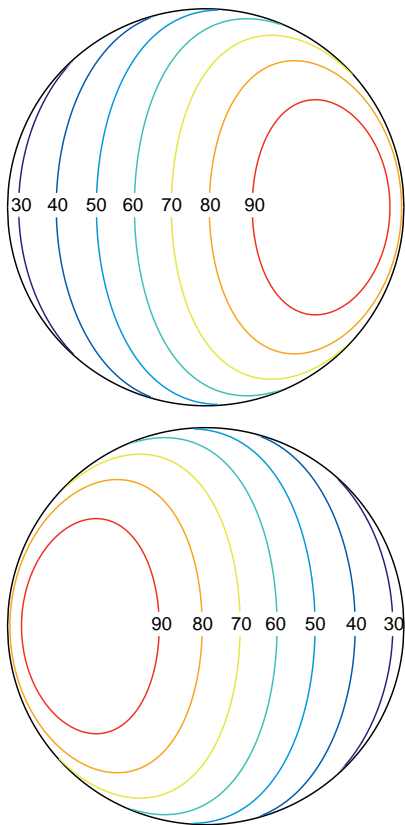


Figure 1. The weighting of the solar disc due to limb darkening and the solar rotation. The top panel shows the results for the instrumental blue wing, while the bottom panel shows the results for the instrumental red wing. The station velocity, v_{st} , is 0 m s^{-1} .

It should be noted that the results shown in Figure 1 have been calculated when $v_{st} + v_{grs} = 0 \text{ m s}^{-1}$. However, the observed bias continually changes as v_{st} varies. In Section 4 we examine how the variations in v_{st} alter the observed bias. However, first we add to this model of the observed inhomogeneity by considering the effect the position of the detector has on the observed bias.

3.1 Weighting of the solar image due to the position of the detector

Consider a vertical slice through the vapour cell (see Figure 2), which is a square of side 15 mm and the port and starboard detectors are positioned on the right- and left-hand sides of the vapour cell respectively. The intensity of light detected from a particular region on the solar disc by the port detector depends on the distance between that region on the image of the Sun in the vapour cell and the inside wall of the vapour cell on the side of the port detector (z in Figure 2). Here we have only considered the perpendicular distance between the region on the image and the wall of the vapour cell. This is not strictly true in a real instrument, which has a system of lenses between the image and the detector, but it does provide a good first-order approximation.

The intensity observed by the detector from a given region on the image of the Sun, I , is determined by the optical depth of the vapour in the cell along the path, τ , and is given by

$$I = I_0 e^{-\tau}, \quad (4)$$

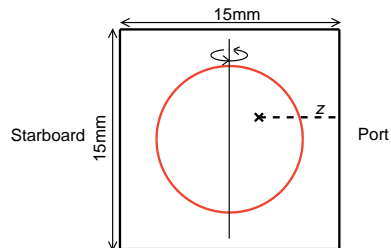


Figure 2. A schematic of a vapour cell. The vapour cell has dimensions $15 \text{ mm} \times 15 \text{ mm}$. At the centre of the vapour cell is the observed image of the Sun (red circle). The port and starboard detectors are positioned on either side of the vapour cell. Here we take the optical path of light to the detector to be horizontal. In this figure the optical path is shown by the dashed line and z is the distance travelled by light through the vapour. Also shown are the axis and direction of rotation. Note that the actual orientation of the rotation axis is dependent on season (see Section 5).

where I_0 is the intensity of light received from the Sun. The optical depth is given by

$$\tau = Kz, \quad (5)$$

where K is the extinction coefficient and z is the horizontal path length (see Figure 2). We have assumed that K is constant throughout the vapour cell and so as z increases I decreases. It should be noted here that this model is based on the assumption that only single scattering is significant. We define τ_0 as the optical depth at the centre of the cell, when $z = 7.5 \text{ mm}$.

We now consider the effect on the weighting of unresolved solar observations of the detector position alone and then we combine this effect with the previously considered results for limb darkening and solar rotation.

3.1.1 Weighting of the solar image observed by the port and starboard detectors

Figure 3 shows the results of considering just the effect of observing on different sides of the vapour cell. As in Figure 1 the most heavily weighted region is given a weighting of 100. The other values of the other contours are then determined as a percentage of the maximum i.e. a contour of 50 means the region contributes half the amount contributed by a region with a contour of 100. Contours with values from 30 to 90 have been plotted. We have assumed that the vapour has an optical depth at the centre of the cell, τ_0 , of unity and so $K = 133.3 \text{ m}^{-1}$. In later sections we change the value of τ_0 (see Sections 4.5, 4.6 and 5). We gave the image of the solar disc in the vapour cell a radius of 5 mm as this is known to be the approximate size the solar image in a BiSON vapour cell. In the remainder of this paper we assume that the centre of the image of the solar disc coincides with the centre of the vapour cell. This is not strictly true for the real BiSON instruments but a shift away from the centre of the cell will not alter the relative weighting across the disc.

The observations are weighted most heavily towards the side of the solar disc that is closest to the detector. Thus, the starboard observations are weighted towards the approaching limb of the Sun, while the port observations are weighted towards the receding limb. As we have only considered the horizontal distance between a pixel on the solar image and the edge of the vapour cell the contours of

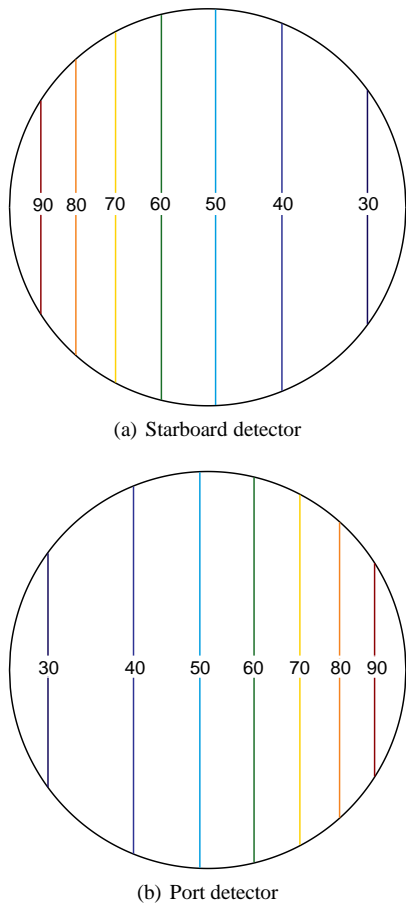


Figure 3. The weighting across the solar disc caused by the positioning of the detector.

constant weighting are vertical lines. It should be noted that the effect of the detector’s position on the observed bias is independent of which instrumental absorption wing is considered, and the station velocity.

We now move on to amalgamate the effects of the Sun’s rotation, limb darkening and the position of the detector.

3.2 Weighting of the solar disc due to the combined effect of the solar rotation, limb darkening and the position of the detector

Figure 4 shows the weighting of the solar disc in Sun-as-a-star Doppler velocity observations when the effects of the solar rotation, limb darkening and the position of the detector are considered and $v_{st} + v_{grs} = 0 \text{ m s}^{-1}$. The values of the contours are defined in the same way as for Figures 1 and 3. Comparison between Figure 4 and Figure 1 implies that the position of the detector is very important to the observed bias across the solar disc. Before the instrumental effect was considered the blue wing observations were weighted towards the receding limb of the Sun (the right-hand limb in Figure 1). When the Sun is observed by the starboard detector the results are shifted towards the approaching solar limb (the left-hand limb in Figure 4). The balance between these two effects results in the observations being weighted most heavily towards the centre of the disc. Similar reasoning can be used to explain why the red, port observations are also weighted towards the centre of the solar disc. Closer inspection reveals that the blue starboard obser-

vations are weighted very slightly towards the approaching limb of the Sun (left-hand limb in Figure 4), while the red port observations are weighted slightly towards the receding solar limb. The results observed in Figure 4 therefore imply that the dominant effect in determining the weighting across the solar disc is that of the position of the detector.

When $v_{st} + v_{grs} = 0 \text{ m s}^{-1}$ the red, starboard map is the mirror image of the blue, port map and the red, port map is the mirror image of the blue, starboard map. As v_{st} increases the weighting patterns are shifted towards the approaching limb of the Sun and so the results are no longer symmetric.

When determining I_r and I_b , and consequently the observed Doppler velocity, v_{obs} , we sum the intensities observed from each region on the solar disc. Therefore, Figure 4 implies that the calculated observed velocity does not represent a uniform average across the whole disc. We have now built up an image of the weighting of the Sun that accounts for the solar rotation, limb darkening and the position of the detector. We move on to investigate how the bias varies with station velocity. We also consider the sensitivity of the inhomogeneity to various inputs involved in the model calculations.

4 THE SENSITIVITY OF THE MODELLED RATIO OF THE INPUT PARAMETERS

The ratio, R , which is given by equation 2, is the raw datum produced from BiSON observations. Using the model of the unresolved Doppler velocity observations described in Section 3 this ratio can be determined for different values of v_{st} .

To determine the sensitivity of the ratio to various input parameters we have calculated the ratio over a range of station velocities and then varied the input parameters one by one. However, we began by determining the ratio when the bias caused by the solar rotation and the limb darkening only were included in the calculations and the results are shown in Figure 5 (black diamonds). As expected, when the sum of v_{st} and v_{grs} is zero (i.e. $v_{st} = -632 \text{ m s}^{-1}$) the blue and red wing observations are symmetric and so the ratio is zero. The ratio increases as v_{st} increases, however, the relationship between v_{st} and R is not linear as the observations become biased towards different portions of the solar absorption line and different regions on the solar surface.

Also plotted in Figure 5 are the ratios observed by the port and starboard detectors. In the calculations the radius of the image of the Sun in the vapour cell was 5 mm and the optical depth, τ_0 , was unity at the centre of the cell. The results show that the ratio is dependent on which detector is considered. The observations made by the port detector are red shifted, while the observations made by the starboard detector are blue shifted. Usually, when dealing with real BiSON data, the mean of the port and starboard ratios is determined. This mean ratio (the solid blue line in Figure 5) is not absolutely identical to the ratio calculated without considering the position of the detector (the black diamonds in Figure 5). The difference between the mean ratio and the detector-independent ratio increases with v_{st} and is of the order of 1 per cent.

We move on to determine the sensitivity of the calculations to the assumed values of various instrumental parameters.

4.1 Sensitivity of the calculations to the width of the solar absorption line

One of the main input parameters in the calculations that determine the ratio is the width of the solar absorption line. To determine the

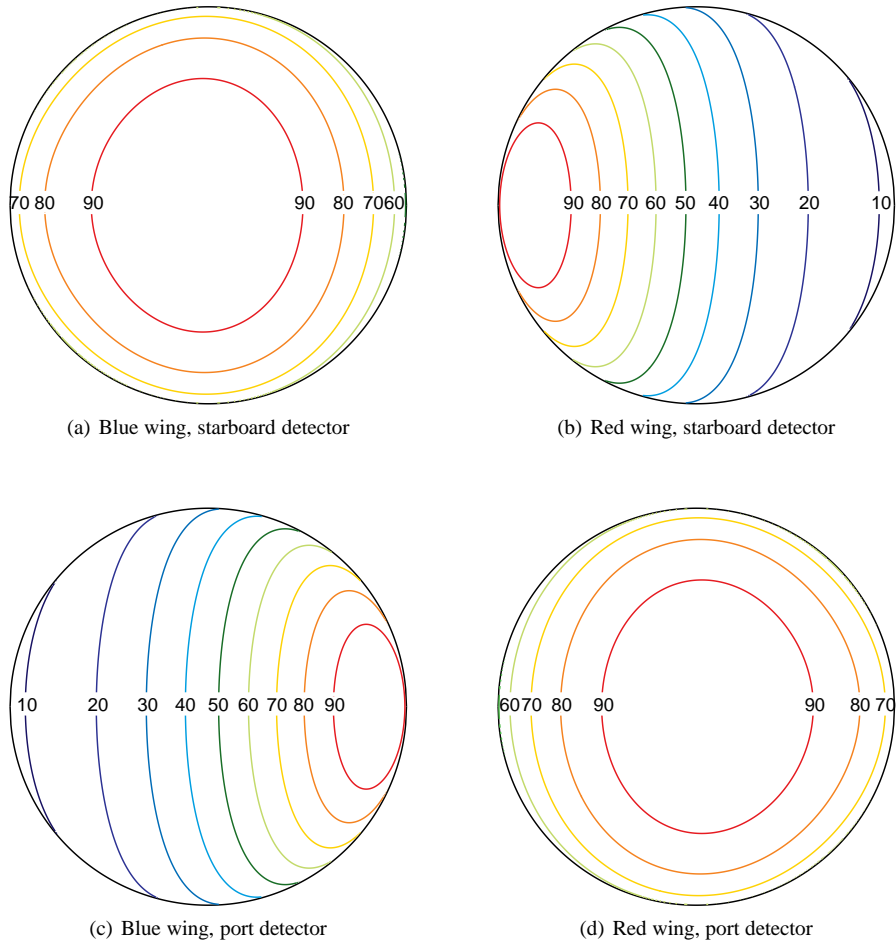


Figure 4. Contour maps showing the weighting of the solar disc that is observed when the position of the detector is considered as well as the limb darkening and the effect of the solar rotation. The radius of the image in the vapour cell is 5 mm, $v_{st} + v_{grs} = 0 \text{ m s}^{-1}$ and the optical depth at the centre of the cell is unity.

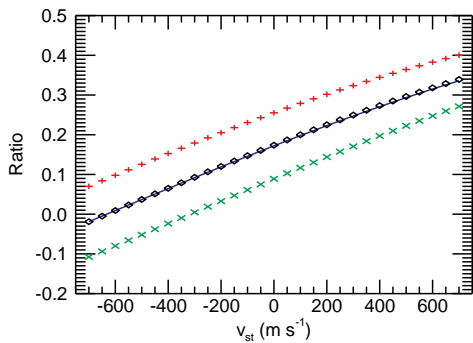


Figure 5. The modelled ratio as a function of station velocity. The black diamonds represent the results when only the effect of rotation and limb darkening are considered. The green crosses represent the starboard observations and the red plus signs represent the port observations. The solid blue line represents the mean of the port and starboard ratios.

weighting across the solar disc we consider the solar absorption line observed from $\sim 250,000$ pixels on the solar disc individually. Each pixel is sufficiently small that the solar absorption line observed from any one pixel will not be noticeably broadened by the solar rotation, unlike a solar absorption line observed from the whole Sun. We have used measurements made by the Themis instrument on Izaña (Simoniello et al. 2008) to estimate the width

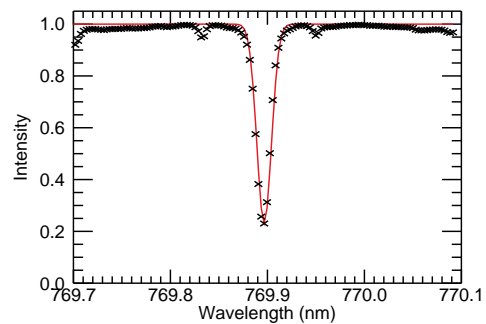


Figure 6. The Fraunhofer line observed by Themis when looking at the centre of the solar disc, where the line-of-sight velocity due to the solar rotation is zero (black crosses). Also plotted is a Gaussian approximation to this line (solid red line).

of a solar potassium absorption line that is observed by a single pixel. Themis makes resolved observations of the solar potassium absorption line from a small pixel at the centre of the solar disc. Consequently, the solar absorption line observed by Themis, which is shown in Figure 6, is not broadened by the solar rotation and so can be used to model the solar absorption line observed from an individual pixel on the Sun. The scanned absorption profile observed by Themis is well approximated by a Gaussian with a full width

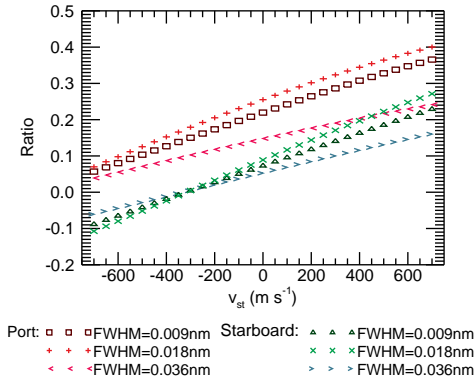


Figure 7. Sensitivity of the modelled ratio to the FWHM of the solar absorption line. The different symbols represent the results calculated using different values of the FWHM of the solar absorption line (see legend).

at half maximum (FWHM) of 0.018 nm (see Figure 6). To investigate the sensitivity of the ratio to the width of the solar absorption line, calculations were performed when the FWHM of the solar absorption line observed by one pixel was increased to 0.036 nm and decreased to 0.009 nm. The results are shown in Figure 7.

The gradient of the variation in the ratio with v_{st} is very sensitive to the assumed FWHM of the solar absorption line. It is, therefore, very important to ensure that the assumed value of the width of the solar absorption line is correct if the ratio is to be modelled accurately. Notice that the gradient is steepest when the FWHM of the solar absorption line is that of the Themis line (0.018 nm). This is because BiSON instruments have been set up so that the observations are as sensitive as possible to any velocity changes. When the FWHM of the solar line is 0.018 nm the instrument measures the intensity of light on the steepest linear parts of the absorption line. However, when the width of the solar line is increased the instrument determines the intensities on the shallow base of the solar line and so is less sensitive to changes in velocity. Similarly, when the FWHM of the solar line is decreased observations are made of the outer parts of the solar line, where the gradient is also less steep and therefore the sensitivity is again decreased.

4.2 Sensitivity of the calculations to the width and separation of the instrumental absorption lines

When calculating the effect of the Sun's rotation on the bias across the solar disc we had to include various parameters that described the instrumental absorption lines. We took the FWHM of these lines to be 700 m s^{-1} (or 0.0018 nm), based on the Doppler broadening expected given the temperature of the vapour cell. We took the separation between the blue and red instrumental wings to be 5200 m s^{-1} (or 0.013 nm), based on the Zeeman splitting expected when the potassium vapour in the cell is placed in a magnetic field of 0.18 T. Here we explore how sensitive the calculations are to variations in the input values of these parameters.

We determined the ratio at different values of v_{st} when the widths of the instrumental absorption lines were increased to 1400 m s^{-1} (or 0.0036 nm). Figure 8 indicates that doubling the width of the instrumental absorption lines alters the calculated ratio by only a small amount. The maximum change in the ratio, which occurs at large v_{st} , is ~ 0.09 , and so this is not an important effect.

Also plotted on Figure 8 are the results obtained when the separation of the instrumental components was decreased to 2600 m s^{-1} (or 0.0067 nm) and increased to 7800 m s^{-1} (or

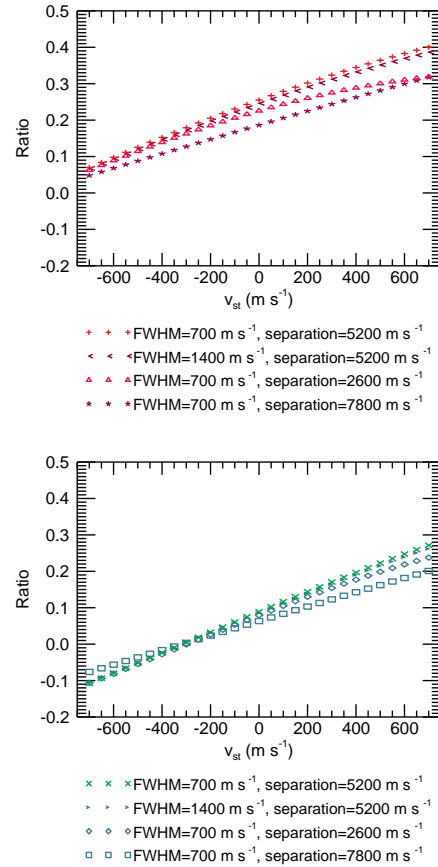


Figure 8. Sensitivity of the modelled ratio to the FWHM and separation of the instrumental absorption lines. The top panel shows the results for the port detector and the bottom panel shows the results for the starboard detector. Each symbol represents different values of the FWHM and separation of the instrumental absorption lines (see legends).

0.0200 nm). In reality this could be achieved by altering the strength of the magnetic field in which the vapour cell is placed. In these calculations the width of the instrumental absorption lines were taken as 700 m s^{-1} . Altering the separation of the instrumental components affects the gradient of the variation of the ratio with v_{st} . Therefore, it is important that the separation of the blue and red instrumental absorption lines is known to allow precise models of the ratio to be made.

4.3 Sensitivity of the calculations to the position angle of the Sun's rotation axis

The position angle of the Sun's rotation axis, P , varies as Earth orbits the Sun and can be tilted by more than 26° from vertical. The observed value of P for any day can be found in a standard almanac. The modelled ratio was determined when the position angle of the Sun's rotation axis was $P = 26^\circ$ and the results are plotted in Figure 9. Note that the change in ratio is independent of the sign of P i.e. the same results were obtained when $P = -26^\circ$. Although only a small effect, the determined ratios are sensitive to the orientation of the Sun's rotation axis and the difference between the port and starboard ratios decreases as $|P|$ increases.

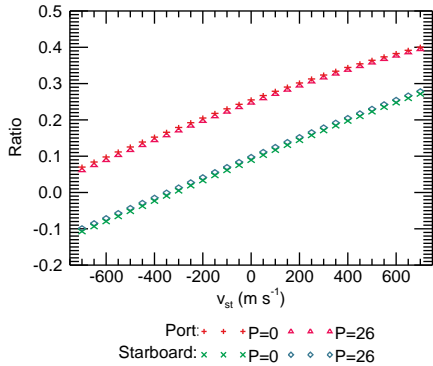


Figure 9. Sensitivity of the modelled ratio to the orientation of the Sun's rotation axis. The results are plotted for $P = 0^\circ$ and $P = 26^\circ$ (see legend).

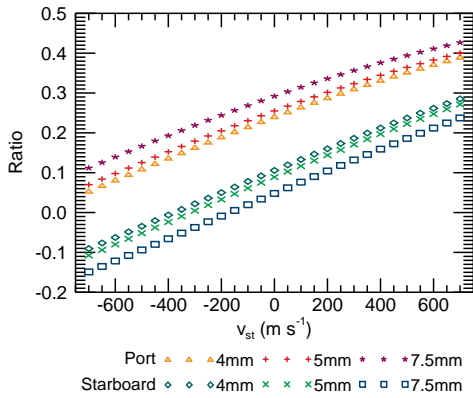


Figure 10. A comparison between the modelled ratio determined for different image radii. The modelled ratio is plotted as a function of station velocity.

4.4 Varying of the size of the solar image

Although the radius of the solar image observed in BiSON instruments is not precisely known it is estimated to be of the order of 4 – 5 mm. Furthermore the observed radius of the Sun varies by ~ 3 per cent throughout the course of a year. Therefore the modelled ratio at different values of v_{st} was determined when the size of the image was 4 mm, 5 mm and 7.5 mm, which is the largest possible radius that the image can have, assuming that the vapour cell observes the whole disc. We have assumed the optical depth at the centre of the vapour cell, τ_0 , is unity. Figure 10 shows that reducing the size of the observed image decreases the difference between the port and starboard ratios. Therefore it is necessary to know the size of the image in the vapour cell if rigorous models of the observed weighted mean velocity are to be made. Even the yearly variation of 3 per cent in the size of the solar image is non-negligible and so must be included when modelling variation in the ratio with time.

4.5 Varying the optical depth of the vapour

We believe that the optical depth, τ_0 , in the vapour cell is of the order of unity. However, the precise optical depth at the centre of the cell is very difficult to determine observationally. Additionally, any small variation in the temperature of the vapour in the cell will alter its optical depth. We therefore investigated the effect of varying the optical depth at the centre of the cell by altering the value of the extinction coefficient, K . Calculations were made when the optical

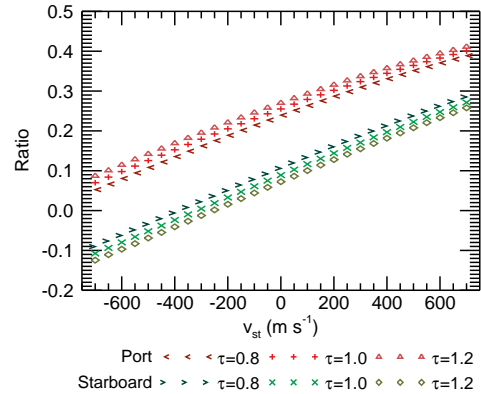


Figure 11. A comparison between the modelled ratio calculated when the optical depth, τ_0 , of the vapour is altered. The modelled ratio is plotted as a function of station velocity.

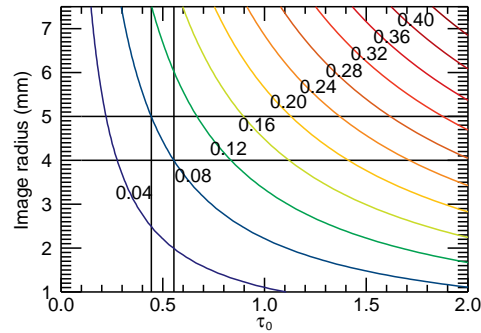


Figure 12. A contour map showing the variation in the difference between the port and starboard ratios with image radius and optical depth, τ_0 .

depth at the centre of the cell, τ_0 , was 0.8, 1.0 and 1.2. The results are plotted in Figure 11. The radius of the solar image in the vapour cell was 5 mm. Changing the optical depth of the vapour has a similar effect on the calculated ratio as altering the size of the image. In fact, varying τ_0 by a value of 0.2 is equivalent to altering the radius of the image by 1 mm. Hence it is also important to know what the optical depth at the centre of the vapour cell is when modelling the ratio observed by unresolved Doppler velocity observations.

4.6 Determining the optical depth in the vapour cell and the radius of the observed image

Figure 12 is a contour map that shows the manner in which the separation of the port and starboard ratios varies with changes to both the optical depth at the centre of the cell and the image radius when $v_{st} = 0 \text{ m s}^{-1}$. Although the magnitude of the offset between the port and starboard ratios is dependent upon which instrument is considered the difference between the ratios is generally of the order of 0.08 when $v_{st} = 0 \text{ m s}^{-1}$. Since the radius of the solar image is believed to be in the range of 4 – 5 mm, Figure 12 implies that the optical depth, τ_0 , is in the range 0.55 – 0.44 (as indicated by the black lines in Figure 12).

We now use the observed daily ratios to determine a velocity offset in the BiSON data and we use the derived information on the vapour cell's optical depth to establish whether or not our model can accurately replicate the observations.

5 VELOCITY OFFSET OBSERVED IN BISON DATA

Equation 3 takes into account the varying values of v_{orb} and v_{spin} and so each value of $R(v_{\text{st}})$ should correspond to the same station velocity from day to day. We have determined the observed velocity intercept that corresponds to a constant value of $R(v_{\text{st}})$ for the port and starboard detectors separately. The ratio, $R(v_{\text{st}})$, was calculated using the daily best fit coefficients, a_i . We have called the determined intercept the velocity offset.

The minimum observed ratio in any one day is often greater than zero. Therefore, to determine the velocity that corresponds to a ratio value of $R(v_{\text{st}}) = 0$ we would have to extrapolate. However, the minimum observed ratio is often less than $R(v_{\text{st}}) = 0.15$ and so the corresponding velocity offset can be found by interpolation. Since the errors associated with interpolation are less than the errors associated with extrapolation we have chosen to find the velocity offset when $R(v_{\text{st}}) = 0.15$.

For any one day the accuracy of the fit, which determines the coefficients, a_i , is improved if more data points are observed. Hence the velocity offset was only determined for days when more than 500 ratios were observed since this constitutes approximately half a day of data.

Figure 13 shows the velocity offset observed by two BiSON instruments as a function of the orbital velocity, v_{orb} . The analysis was performed for different instruments (and, although not shown here, different years) to ensure the observed effects were not instrument (or year) specific. The results are very similar for both sites and the offset is observed to vary in a similar manner from year to year. Figure 13 shows that the value of the velocity offset not only varies with v_{orb} , but the magnitude of the offset and the shape of the variation are dependent on which detector is considered. It should be noted that the offset observed in the mean of the port and starboard data shows less variation than when the two detectors are considered individually.

The process for determining the velocity offset in the BiSON data was repeated using model data that takes into account the bias across the disc due to the solar rotation, limb darkening and the position of the detector. When creating the model data the optical depth at the centre of the vapour cell was taken to be 0.55. The radius of the image was varied throughout the year in a sinusoidal manner and had a maximum radius, in January, of 4 mm. The orientation of the model Sun's rotation axis was varied sinusoidally between $\pm 26.3^\circ$ throughout the simulated year.

Figure 14 shows the modelled velocity offset. Comparison between Figure 13 and Figure 14 indicates that the model is able to replicate the approximate magnitudes of the offsets, the separation between the port and starboard offsets and the general shape of the offsets. However, the variation in the modelled port offsets is approximately a factor of 2 smaller than the variation in the observed port offsets and the same is true for the starboard offsets. The variation that is visible in the modelled offsets is introduced primarily because the orientation of the Sun's rotation axis varies with time. It is possible that a systematic variation in other parameters such as the temperature, and consequently the optical depth, of the vapour in the cell could also contribute to the observed variation in the offsets. Furthermore, any variations in the orientation of the image of the Sun in the vapour cell because of instrumental effects will alter the observed offsets. The presence of these offsets in the BiSON data is important for the long term stability of the data, which ultimately affects the quality of the data.

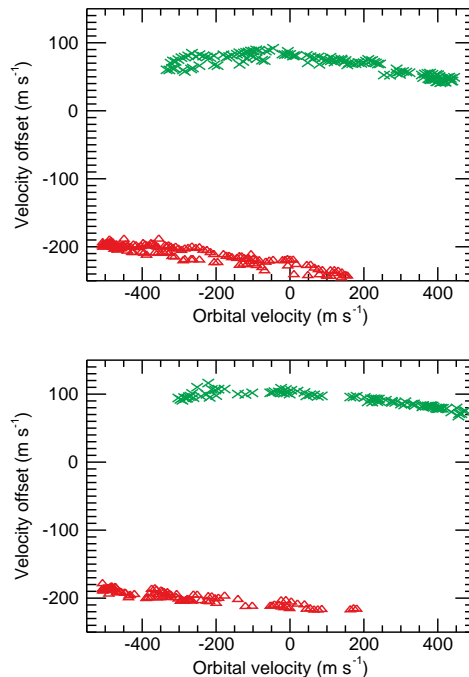


Figure 13. Top panel: The velocity offset observed in Las Campanas data in 2006 as a function of v_{orb} . Bottom panel: The velocity offset observed in Narrabri data in 2006 as a function of v_{orb} . In each panel the red triangles represent the results from the port detector, while the green crosses show the velocity offset observed by the starboard detector.

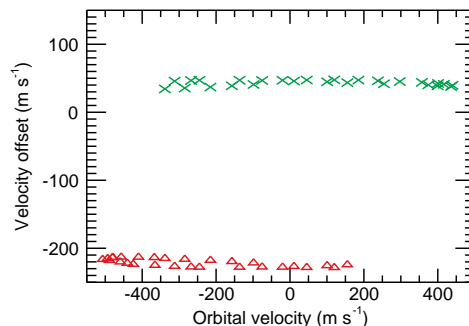


Figure 14. The modelled velocity offset as a function of v_{orb} . The red diamonds represent the results from the port detector, while the green crosses show the velocity offset observed by the starboard detector.

6 DISCUSSION

We have shown that the observed Doppler imaging across the solar disc is different for the red and blue wing observations and the port and starboard observations. This means that the observations are biased towards different portions of the solar Fraunhofer line. From the centre of a solar absorption line to its wings the height of formation in the solar atmosphere varies by hundreds of kilometres. Therefore the port and starboard detectors measure velocities at different depths in the solar atmosphere and so the realization of the solar noise observed by each detector will be only partially correlated. Furthermore, the observed amplitudes of solar oscillations are dependent on the depth in the atmosphere at which the observations are made and consequently the amplitudes of the modes observed by each instrument will be different. The variation in observation depth could impact on models of mode excitation as the

excitation rate is dependent on the mode mass, which, to correctly match the observations must be determined at the height at which the observations are made (Baudin et al. 2005).

Another consequence of the observed weighting across the solar disc is the effect on the visibility of the modes. The visibility of a mode varies depending on the sensitivity of the observing instrument's response over the solar disc to a mode's eigenfunction. Christensen-Dalsgaard (1989) considered the manner in which the visibilities of modes in unresolved observations are affected by the solar rotation and limb darkening. Since the position of the detector has a significant influence on the weighting across the solar disc this too should be considered when determining the visibility of modes. Furthermore, as the observed bias is dependent on v_{st} , which varies with time, the visibility of the modes will also be time dependent.

The observed Doppler imaging is sensitive to many different input parameters. However, we have shown that the instruments have been well calibrated to be sensitive to small changes in the line-of-sight velocity. We have been able to use the separation of the port and starboard ratios to estimate the Doppler imaging in the cell. The difference between the port and starboard ratios in the modelled and observed data are in agreement when the size of the solar image in the vapour cell is 4 mm and the optical depth at the centre of the vapour cell, τ_0 is 0.55. The true values of the size of the image and the optical depth in the vapour cell are not known precisely. As the observed ratio is sensitive to the optical depth (see Figures 11 and 12) this work highlights the need to determine the value of the optical depth in the vapour cell and work within the BiSON group is ongoing to this effect.

The sensitivity of the Doppler imaging to input parameters such as the position angle of the Sun's rotation axis means that a velocity offset is introduced into the BiSON data. Moderate agreement has been achieved between the observed and modelled velocity offsets. However, we believe there is a further effect that is related to a variation in the tilt of the instrument that could explain the difference between the observations and the model. The presence of a velocity offset introduces low-frequency noise to the BiSON data. We have shown that this offset can potentially be modelled and can, therefore, in principle be removed from the data, thereby reducing the observed level of noise. The introduced noise has a $1/\text{frequency}$ dependence and so it is particularly important at very low frequencies. Therefore, removing this noise source make it easier to observe low-frequency p modes and g modes in Sun-as-a-star data.

ACKNOWLEDGEMENTS

We are grateful to R. Simoniello for allowing us to use Themis data. This paper utilizes data collected by the Birmingham Solar-Oscillations Network (BiSON). We thank the members of the BiSON team, both past and present, for their technical and analysis support. We also thank P. Whitelock and P. Fourie at SAAO, the Carnegie Institution of Washington, the Australia Telescope National Facility (CSIRO), E.J. Rhodes (Mt. Wilson, California) and members (past and present) of the IAC, Tenerife. BiSON is funded by the Science and Technology Facilities Council (STFC). The authors also acknowledge the financial support of STFC.

REFERENCES

- Boumier P., Chaplin W. J., Gouttebroze P., 2005, *A&A*, 433, 349
 Brookes J., Isaak G., van der Raay H., 1978a, *MNRAS*, 185, 19
 Brookes J., Isaak G., van der Raay H., 1978b, *MNRAS*, 185, 1
 Christensen-Dalsgaard J., 1989, *MNRAS*, 239, 977
 Elsworth Y., Howe R., Isaak G. R., McLeod C. P., Miller B. A., New R., Wheeler S. J., 1995, *A&AS*, 113, 379
 Simoniello R., Jiménez-Reyes S. J., García R. A., Pallé P. L., 2008, *Astronomische Nachrichten*, 329, 494